

Dominant Carbapenemase-Encoding Plasmids in Clinical Enterobacterales Isolates and Hypervirulent *Klebsiella pneumoniae*, Singapore

Melvin Yong, Yahua Chen, Guodong Oo, Kai Ching Chang, Wilson H.W. Chu, Jeanette Teo, Indumathi Venkatachalam, Natascha May Thevasagayam, Prakki S. Rama Sridatta, Vanessa Koh, Andrés E. Marcoleta, Hanrong Chen, Niranjan Nagarajan, Marimuthu Kalisvar, Oon Tek Ng, Yunn-Hwen Gan

Dissemination of carbapenemase-encoding plasmids by horizontal gene transfer in multidrug-resistant bacteria is the major driver of rising carbapenem-resistance, but the conjugative mechanics and evolution of clinically relevant plasmids are not yet clear. We performed whole-genome sequencing on 1,215 clinical Enterobacterales isolates collected in Singapore during 2010–2015. We identified 1,126 carbapenemase-encoding plasmids and discovered pKPC2 is becoming the dominant plasmid in Singapore, overtaking an earlier dominant plasmid, pNDM1. pKPC2 frequently conjugates with many Enterobacterales species, including hypervirulent *Klebsiella pneumoniae*, and maintains stability in vitro without selection pressure and minimal adaptive sequence changes. Furthermore, capsule and decreasing taxonomic relatedness between donor and recipient pairs are greater conjugation barriers for pNDM1 than pKPC2. The low fitness costs pKPC2 exerts in Enterobacterales species indicate previously undetected carriage selection in other ecological settings. The ease of conjugation and stability of pKPC2 in hypervirulent *K. pneumoniae* could fuel spread into the community.

Author affiliations: National University of Singapore, Singapore (M. Yong, Y. Chen, G. Oo, K.C. Chang, W.H.W. Chu, N. Nagarajan, M. Kalisvar, Y.-H. Gan); National University Hospital, Singapore (J. Teo); Singapore General Hospital, Singapore (I. Venkatachalam); National Centre for Infectious Diseases, Singapore (N.M. Thevasagayam, P.S.R. Sridatta, V. Koh, M. Kalisvar, O.T. Ng); Tan Tock Seng Hospital, Singapore (V. Koh, M. Kalisvar, O.T. Ng); Universidad de Chile, Santiago, Chile (A.E. Marcoleta); Genome Institute of Singapore, Singapore (H. Chen, N. Nagarajan); Nanyang Technological University, Singapore (O.T. Ng)

DOI: <https://doi.org/10.3201/eid2808.212542>

The global rise of carbapenem-resistant Enterobacterales (CRE) infections is posing a grave challenge to hospital systems worldwide (1). Carbapenemase genes usually are located on plasmids that can transmit vertically along clonal lineages and horizontally between different strains and species (2). However, the principles governing the transmission of carbapenemase-encoding plasmids in clinically relevant settings are complex and dynamic. Plasmid properties, donor, recipient, and ecologic factors all affect transmission (3,4).

Previously, we found a 71,861-bp pKPC2 plasmid, pKPC2_sg1 (GenBank accession no. MN542377), in all 18 carbapenem-resistant hypervirulent *Klebsiella pneumoniae* isolates available in the Carbapenemase-Producing Enterobacteriaceae in Singapore (CaPES) collection (5,6). (Enterobacteriaceae is the former name of Enterobacterales.) The plasmid sequence was stable and unchanged after moving into different bacterial hosts or when maintained in human hosts for >200 days. This discovery prompted questions about the extent of pKPC2_sg1 dominance in clinical settings in Singapore, and its transmissibility and stability in hypervirulent *K. pneumoniae*. Using >1,000 CRE isolates collected from the 6 public hospitals in Singapore during 2010–2015, a subset of which was previously described (6), we examined the distribution of different carbapenem-encoding plasmids to investigate the dynamics and dominance of pKPC2.

Materials and Methods

Bacterial Strains, Growth Conditions, and Plasmids

We analyzed 1,215 CRE isolates for carbapenemase plasmids distribution (Appendix 1 Table,

<https://wwwnc.cdc.gov/EID/article/28/8/21-2542-App1.xlsx>). We have included information on modified and unmodified plasmids, bacterial mutant generation and the Enterobacterales strains (Appendix 2, <https://wwwnc.cdc.gov/EID/article/28/8/21-2542-App2.pdf>). Unless otherwise specified, we grew strains on Lennox L Agar lysogeny agar (LA) (Invitrogen-ThermoFisher, <https://www.thermo-fisher.com>) at 37°C overnight before the assays.

Whole-Genome Sequencing

We performed whole-genome sequencing (WGS) by using the MiSeq platform (Illumina, <https://www.illumina.com>) and the GridION X5 system (Oxford Nanopore Technologies, <https://nanoporetech.com>). To assemble genomes, we used SPAdes Genome Assembler version 3.11.1 (7) and Unicycler version 0.4.8 (8). For bacterial species assignment, we performed multilocus sequence typing (MLST) by using Bacterial Isolate Genome Sequence Database version 2.8 (9) or the Center for Genomic Epidemiology Bacterial Analysis Pipeline (<https://www.genomepidemiology.org>) and Kraken (10). We identified antimicrobial resistance genes in CRE isolates by using Abricate version 1.0.1 (11) and the National Center for Biotechnology Information (NCBI) Bacterial Antimicrobial Resistance Reference Gene Database (12). We identified virulence genes by using the Virulence Factor Database (13) (Appendix 2).

Plasmid Annotation and Analysis

We analyzed the pKPC2 sequence (GenBank accession no. MN542377) by using GeneMarkS (14) to acquire a list of predicted protein sequences and subjected sequences to blastp (14). We used blastp results to annotate genes on the plasmid, which we drew by using the BLAST Ring Image Generator (15). We also analyzed the plasmid sequence by using Plasmid-Finder version 2.1 (16,17).

Replicon Analysis

We used *EcoRI* and *BamHI* restriction enzymes to double digest pKPC2 DNA for 1 hour at 37°C, then ligated the fragments to the pR6K plasmid by using T4 DNA Ligase (Promega, <https://www.promega.com>). We then used *Escherichia coli* Stellar HST08 Competent Cells (TaKaRa Bio, Inc., <http://www.takara-bio.com>) to introduce fragments through heat shock, and selected the transformants on LA with kanamycin (50 µg/mL). However, pR6K cannot replicate in HST08 cells because the R6K replicon protein must be provided in trans via lambda *pir*. Only pR6K with ligated fragments carrying a functional replicon can replicate.

We harvested plasmids from the selected clones and submitted these to 1st BASE (<https://base-asia.com>) for Sanger sequencing to determine the inserts. We performed phylogenetic analysis on the identified *trfA* replicon by using ClustalW (<https://www.clustal.org>) and the maximum-likelihood method in MEGA-X version 10.2.6 (18).

Bacterial Growth Assay

We streaked bacterial strains on LA containing antimicrobial drugs for various plasmids: 256 µg/mL erythromycin for pKPC2; 0.5 µg/mL meropenem for pNDM1; and 50 µg/mL kanamycin for pKPC2^{KmR} or pNDM1^{KmR}. We incubated plates at 37°C overnight, then inoculated colonies into Lennox L Broth Base lysogeny broth (LB; Invitrogen-ThermoFisher) containing the same antimicrobial drugs and placed in a shaking incubator set at 37°C and 150 rpm overnight. We measured the optical density at 600 nm (optical density 600) of overnight bacterial culture and recorded the reading before diluting it to 0.001. We added 200 µL of diluted cultures to a 96-well plate and placed these on a Synergy H1 plate reader (BioTek, <https://www.biotek.com>) at 37°C. We measured absorbance at optical density 600 hourly for 24 hours.

Conjugation Experiments

We performed conjugation on 0.22 µm Cellulose Nitrate Filter (Sartorius, <https://www.sartorius.com>) nitrocellulose membranes using a 1:1 ratio of donor to recipient strains on LA. We measured plasmid transfer kinetics from *E. coli* MG1655 at various timepoints up to 4 hours at 37°C. We selected recipient strains on LA; *E. coli* SLC-568 with 50 µg/mL kanamycin or *K. pneumoniae* SGH10 with 40 µg/mL fosfomycin. We used the same antimicrobial drugs to select transconjugants on LA plus 256 µg/mL erythromycin for pKPC2 or 0.5 µg/mL meropenem for pNDM1. For conjugation assays of pKPC2^{KmR} and pNDM1^{KmR}, recipients carried pACYC184^{CmR} for selection. We selected transconjugants on LA with 50 µg/mL chloramphenicol and 50 µg/mL kanamycin and selected recipients without kanamycin. For conjugation into hypervirulent *K. pneumoniae* recipients, we replaced chloramphenicol with 40 µg/mL fosfomycin. We measured conjugation frequency by dividing the number of transconjugants by the number of recipients.

Plasmid Stability Assessment

We cultured strains in LB and 50 µg/mL kanamycin overnight, then subcultured every day by inoculating 4.88 µL of the culture into 5 mL of antimicrobial-free LB, as described (19). At generations 0, 30, 60, and 90,

we serially diluted bacterial cultures and plated on LA with and without 50 µg/mL kanamycin. We further subcultured selected bacterial strains to 300 generations and plated at generation 100, 200, and 300. We calculated plasmid stability as the number of antimicrobial-resistant bacteria per total bacterial count.

To test for plasmid incompatibility, we measured the stability of pKPC2^{KmR} in *E. coli* MG1655 harboring both pKPC2^{KmR} and pRK2-AraE as described (20), except we first grew the strain in LB with both 35 µg/mL gentamicin and 50 µg/mL kanamycin before subculturing for 100 generations in LB with 35 µg/mL gentamicin to select for pRK2-AraE. At every 10th generation, we plated the cultures on LA with 35 µg/mL gentamicin, and LA with 35 µg/mL gentamicin and 50 µg/mL kanamycin.

Regression Analysis

To study the effect of taxonomic relatedness on pKPC2 and pNDM1 conjugation frequencies, we

applied a survival-analysis approach (21). We modeled the donor-recipient pair as a random effect to account for unobserved heterogeneity specific to each pair (Appendix 2).

Results

Dominant Carbapenemase-Encoding Plasmid

From 1,312 CRE isolates (817 unique patients) submitted during September 2010–April 2015 as part of mandatory reporting to the National Public Health Laboratory, we successfully cultured, performed WGS on, and assembled genomes for 1,302 (99.2%) isolates. Of those, 1,251 (96.1%) identified bacterial species and carbapenemase genes were concordant with laboratory data (MIC >1 mg/L or disc diffusion zone diameter <23 mm for imipenem and meropenem) (6). We excluded 36 isolates because patient or date of culture information was missing; thus, we analyzed 1,215 (93.3%) isolates (Figure 1; Appendix

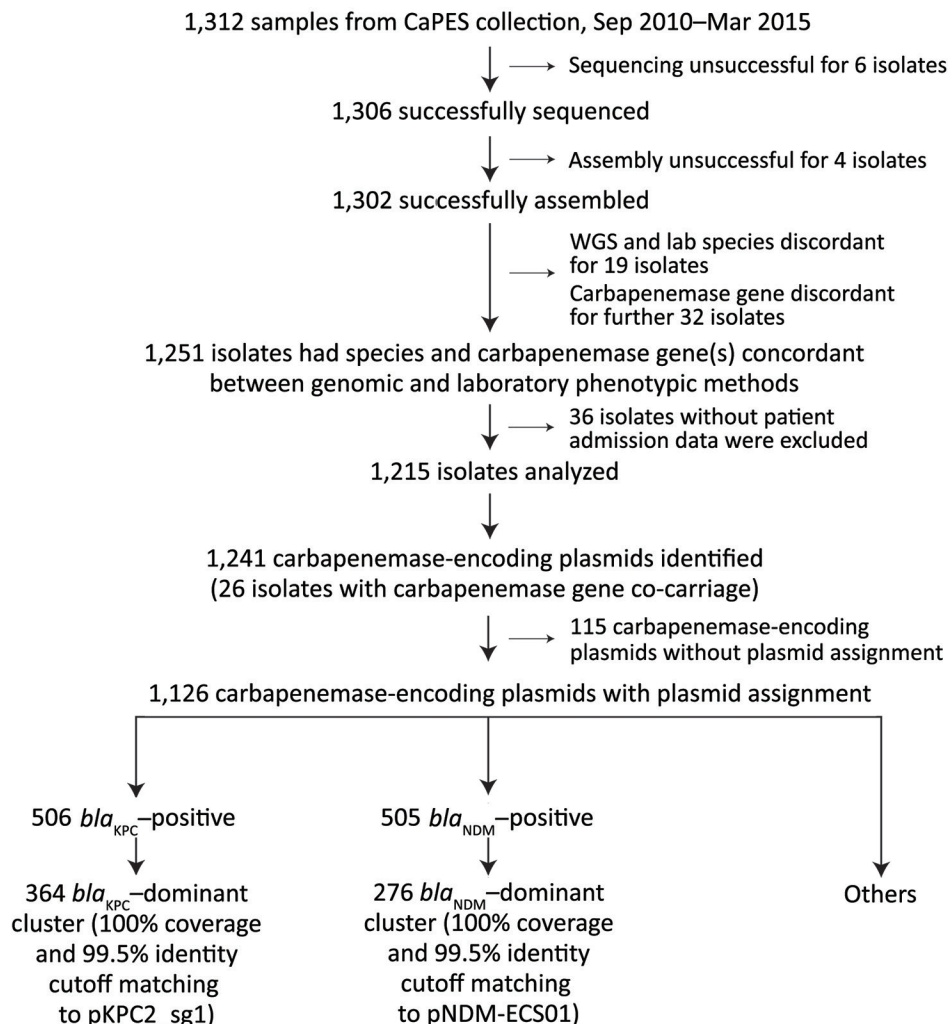


Figure 1. Flowchart of steps used for identifying dominant carbapenemase-encoding plasmids in clinical Enterobacteriales isolates and hypervirulent *Klebsiella pneumoniae*, Singapore. We collected 1,312 samples available in the CaPES collection and analyzed 1,215 whole-genome sequenced samples. We identified 2 dominant clusters with large numbers of carbapenemase-encoding plasmids; the *bla*_{KPC}-dominant cluster comprised pKPC2 plasmids and the *bla*_{NDM}-dominant cluster comprised pNDM1 plasmids. CaPES, Carbapenemase-Producing Enterobacteriaceae in Singapore (CaPES) (Enterobacteriaceae is the former name of Enterobacteriales); WGS, whole-genome sequencing.

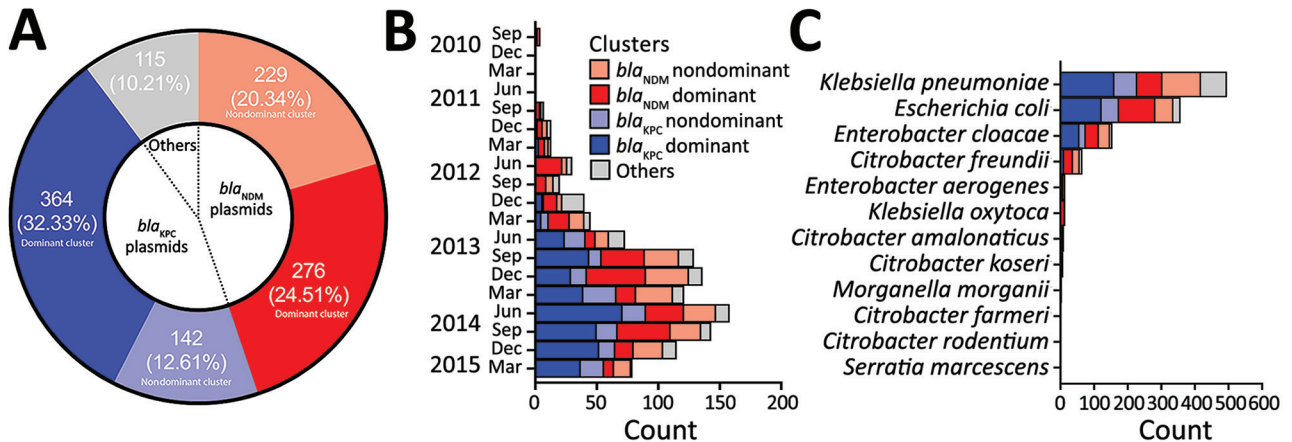


Figure 2. Percentage and distribution of dominant carbapenemase-encoding plasmids in clinical Enterobacteriales isolates and hypervirulent *Klebsiella pneumoniae*, Singapore. A) Percentage distribution of the total carbapenemase-encoding plasmids identified. The bla_{KPC} dominant cluster refers to those harboring pKPC2 plasmid; bla_{NDM} dominant cluster refers to those harboring pNDM1 plasmid. Others indicate carbapenemase-encoding plasmids that do not carry bla_{KPC} or bla_{NDM} . B, C) Distribution of carbapenemase-encoding plasmids identified among Carbapenemase-Producing Enterobacteriaceae in Singapore (CaPES) (Enterobacteriaceae is the former name of Enterobacteriales) samples collected during September 2010–March 2015 (B) and among Enterobacteriales isolates (C). Nondominant cluster refers to other plasmids carrying bla_{KPC} or bla_{NDM} . We found that pKPC2 was the most dominant carbapenemase-encoding plasmid in Singapore during 2010–2015.

1). We successfully identified 1,126 carbapenemase-encoding plasmids with assignments from the 1,215 isolates. We found 2 dominant carbapenemase-encoding plasmids: bla_{KPC} ($n = 506$; 44.94%) and bla_{NDM} ($n = 505$; 44.85%) (Figure 2, panel A). Among the 506 bla_{KPC} plasmids, 364 (32.33%) were pKPC2 plasmids, which we termed the bla_{KPC} -dominant cluster. Among the 505 bla_{NDM} plasmids, 276 (24.51%) were pNDM1 plasmids, which we termed the bla_{NDM} -dominant cluster. Nondominant plasmids included other bla_{KPC} or bla_{NDM} plasmids that did not fall into the pKPC2 or pNDM1 dominant clusters.

During 2010–2012, pNDM1 was predominant but pKPC2 subsequently caught up during 2013–2015 (Figure 2, panel B; Appendix 2 Figure 1, panel A). Those plasmids were largely found in 3 species: *K. pneumoniae* (43.96%), *E. coli* (31.71%), and *Enterobacter cloacae* (13.68%) (Figure 2, panel C). Bacterial sequence type (ST) distribution among bla_{KPC} -positive and bla_{NDM} -positive isolates showed that both bla_{KPC} and bla_{NDM} plasmids were widely distributed across numerous STs, particularly in *K. pneumoniae* (Appendix 2 Figure 1, panel B), indicating that widespread distribution is unlikely due to selective clonal expansion events. The bla_{KPC} -dominant cluster also had more unique isolates than the other clusters, suggesting wider bla_{KPC} transmission (Figure 3).

Evolution of pKPC2 Features

Annotated features on the pKPC2 plasmid map show conjugative genes from the *tra* and *trb* operons and

complete conjugative machinery (Figure 4, panel A). A comparison against the GenBank database for similar plasmids revealed pKPC2 is a hybrid of pSA20021456.2-like plasmids (GenBank accession no. CP030221), with 74% coverage and 99.60% identity, and pKPCAPSS-like plasmids (GenBank accession no. KP008371), with 34% coverage and 99.99% identity (Figure 4, panel A). The conjugative and

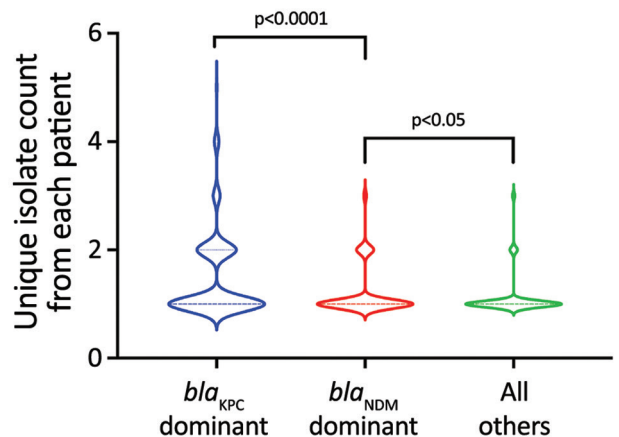
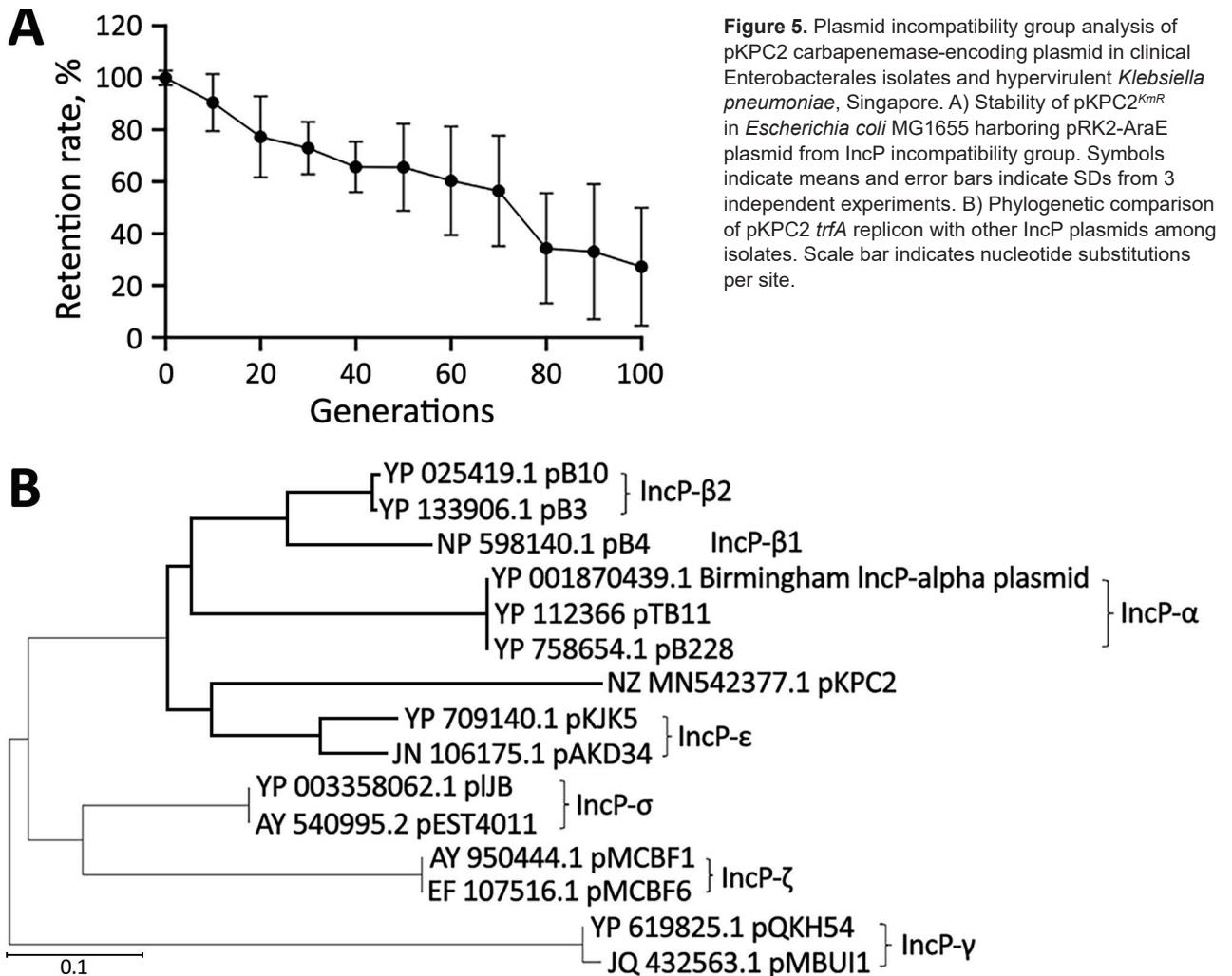


Figure 3. Violin plots showing the unique isolate counts from each patient in a study of dominant carbapenemase-encoding plasmids in clinical Enterobacteriales isolates and hypervirulent *Klebsiella pneumoniae*, Singapore. Unique isolates were defined as different species or different sequence types from same species. We separated unique isolates into 3 groups: bla_{KPC} dominant ($n = 196$), bla_{NDM} dominant ($n = 203$), and all others ($n = 504$), which included bla_{KPC} nondominant, bla_{NDM} nondominant, and others. Brackets indicate p values for nonparametric Mann-Whitney tests between groups.



Stability and Genetic Adaptation of pKPC2 In Vitro

pKPC2 exhibited faster conjugation kinetics, reaching nearly 10^0 after 2–3 hours, than did pNDM1 (GenBank accession no. JADPQD010000004), which took 3–4 hours to reach 10^0 (Figure 6, panel A). With hypervirulent *K. pneumoniae* SGH10 as the recipient, the conjugation frequency remained higher for pKPC2 than for pNDM1 (Figure 6, panel B).

To determine whether those plasmids exert any fitness cost on host strains, we measured the growth rate of host strains in presence or absence of the plasmids. We included plasmids tagged with kanamycin resistance, pKPC2^{KmR} and pNDM1^{KmR}, because they were used for subsequent experiments with kanamycin as a robust selection marker. We found no significant difference in growth rate for *E. coli* MG1655 or *K. pneumoniae* SGH10 (Figure 6, panels C, D). To simulate a nutrient-poor condition, we tested growth rates in minimal media, which also showed

no significant growth differences (Appendix 2 Figure 5). Furthermore, both plasmids remained stable for up to 300 generations without selection pressure (Figure 6, panels E, F). We compared the sequences of the 9 pKPC2^{KmR} plasmids from the 300th generation (pKPC2^{KmR}_Gen300) *K. pneumoniae* SGH10 isolates to the original pKPC2^{KmR} plasmid using in vitro plasmid evolution experiments and noted no major changes in the plasmid sequence (Appendix 2 Figure 6). Among the nine 300th-generation plasmids, 6 had 2 or 4 nucleotide mismatches on β -lactamase genes. However, sequence comparison of the pKPC2 and pKPC2^{KmR} used in this study to the pKPC2_sg1 from the clinical isolate *K. pneumoniae* ENT494 (GenBank accession no. MN542377) shows the same nucleotide polymorphism in the same genes (Appendix 2 Figure 7), indicating that these are likely the only bona fide evolved adaptations of the plasmid. Because host bacteria can also evolve to adapt to plasmid car-

riage (28), we compared the genomic sequences of nine 300th-generation *K. pneumoniae* SGH10 isolates carrying pKPC2 and nine 300th-generation isolates without pKPC2. We hypothesized that host adaptation would lead to an increased number of non-synonymous mutations in the strains carrying the plasmid versus the plasmid-null strains, leading to changes in protein function. However, our results indicated similar numbers of synonymous, non-synonymous, and total nucleotide polymorphism differences in both groups.

pKPC2 Conjugation Frequency and Stability in Enterobacteriales Species

We hypothesize that the predominance of pKPC2 in our clinical isolates is due to its high conjugation frequency to different Enterobacteriales species. The conjugation frequency of pKPC2^{KmR} from MG1655 to other *E. coli* or *E. cloacae* recipient strains were remarkably high, ranging from 10⁻¹ to 10⁰ (Appendix 2 Figure 8, panel A). We observed the same

conjugation frequency for several clinical *Klebsiella* strains, such as *K. pneumoniae* NUH29, *K. quasipneumoniae* TTSH4, *K. oxytoca* 8071169380, and *K. varicola* NUH59. However, some *Klebsiella* recipient strains exhibited lower conjugation frequency, in the 10⁻³ to 10⁻¹ range. For pNDM1^{KmR}, the conjugation frequency was ≈10–100-fold lower than for pKPC2^{KmR} for most pairs. When we used *K. pneumoniae* SGH10 as the donor to the same panel of Enterobacteriales recipients, the conjugation frequency of both plasmids was 10–100-fold lower than when *E. coli* MG1655 was the donor (Appendix 2 Figure 8, panel B). We then swapped the donor-recipient pairs by using the panel of Enterobacteriales strains as donors and *K. pneumoniae* SGH10 as the recipient (Appendix 2 Figure 8, panel C). Overall, the conjugation frequency for pKPC2^{KmR} remained higher than the frequency for pNDM1^{KmR} in most donor-recipient pairs. However, the conjugation frequency of the swapped donor-recipient pairs was not the same as the original pairs, indicating the effects of

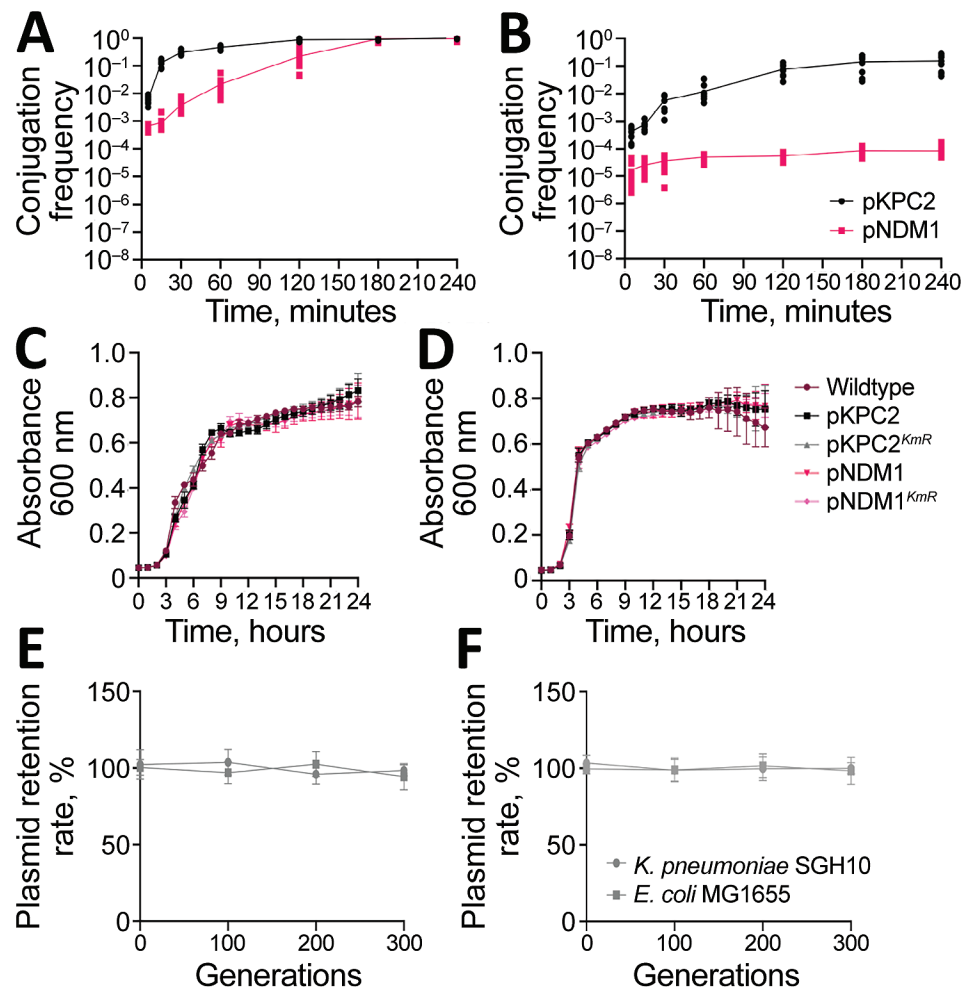


Figure 6. Characterization of pKPC2 carbapenemase-encoding plasmid in clinical Enterobacteriales isolates and hypervirulent *Klebsiella pneumoniae*, Singapore. A, B) Conjugation kinetics of pKPC2 and pNDM1 from *Escherichia coli* MG1655 (donor) to *E. coli* SLC-568 (recipient) (A) or to *K. pneumoniae* SGH10 (recipient) (B). The donor-recipient pairs were mixed in 1:1 ratio and conjugated for 4 hours at 37°C using filter matings. The number of transconjugant and recipient pairs were enumerated by plating. Results from 3 independent experiments were plotted as the conjugation frequency (transconjugant/recipient) over time (minutes). Error bars indicate SDs from 3 independent experiments. C, D) Representative growth curve of *E. coli* MG1655 (C) or *K. pneumoniae* SGH10 (D) with or without plasmids pKPC2, pKPC2^{KmR}, pNDM1, pNDM1^{KmR} grown in LB media at 37°C for 24 h. E, F) Stability of pKPC2^{KmR} (E) and pNDM1^{KmR} (F) in *K. pneumoniae* SGH10 and *E. coli* MG1655 grown in LB up to generation 300. Symbols indicate means and error bars indicate SDs from 3 independent experiments. LB, lysogeny broth.

donor and recipient factors. Both plasmids within the Enterobacterales strains were stable for up to 90 generations, except for *E. coli* UTI89, which failed to retain the pKPC2^{KmR} plasmid (Appendix 2 Figure 8, panels D, E). These results align with clinical data showing the persistence of the pKPC2 plasmid over several months in patients without antimicrobial drug exposure (5).

Conjugation Frequency and Stability of pKPC2 in Hypervirulent *K. pneumoniae*

Because pKPC2 was previously found in 18 local clinical hypervirulent *K. pneumoniae* isolates of K1, K2, and K20 capsular serotypes (5), we hypothesize that the plasmid does not face constraints in transmission to hypervirulent *K. pneumoniae*. Those isolates were loosely defined as hypervirulent *K. pneumoniae* based on occurrence of ≥ 2 virulence genes, such as *iro* and *rmpA* (Appendix 2 Table 1). Indeed, we observed high conjugation frequency for K1 strains (Appendix 2 Figure 9, panel A). On the other hand, K2 and K5 strains exhibited heterogeneity in their plasmid acceptance. However, plasmid conjugation success was independent of capsular types because we observed low conjugation frequency in 2 STs, K2/ST2039 and K5/ST60, whereas other STs of the same capsular type exhibited markedly higher conjugation frequency. Compared with pNDM1^{KmR} (Appendix 2 Figure 9, panel B), the conjugation frequency of pKPC2^{KmR} was ≈ 10 –100-fold higher. In fact, K2/ST2039 and K5/ST60 strains were low conjugators for both plasmids. Despite the low conjugation frequency, the plasmids maintained stability over 90 generations (Appendix 2 Figure 10).

Effects of Taxonomic Factors on pNDM1 Conjugation

To examine the influence of taxonomic factors on pKPC2 and pNDM1 conjugation frequencies, we performed statistical analyses on available datasets (Appendix 2 Figures 8, 9) by using a survival-analysis approach (21). Comparing the baseline conjugation frequency between the same strain, we noted a statistically significant decrease in pKPC2 transfer between the same species (24.0-fold) or same genus (10.2-fold) but no statistically significant decrease between different genera (Table 1). On the other hand, we noted a statistically significant decrease in pNDM1 transfer between the same species (36.3-fold), same genus (123.0-fold), and different genera (87.1-fold). These results suggest that taxonomic factors have a higher influence on pNDM1 than pKPC2, which is especially notable for transfer between the same genus or different genera.

Effect of Bacterial Capsule on Plasmid Conjugation

We examined a panel of isogenic deletion mutants of *K. pneumoniae* SGH10 as recipients that could affect donor-recipient pair mating dynamics. Conjugation frequency was enhanced in $\Delta rmpA$ and $\Delta ICEp10$ recipients, but the greatest impediment to plasmid conjugation was the capsule (Appendix 2 Figure 9, panel C). The $\Delta wcaJ$ recipient exhibited conjugation efficiency approaching 10^0 for both plasmids (Appendix 2 Figure 9, panel D). Similarly, capsule absence increased the conjugation frequency of both plasmids from *E. coli* MG1655 to capsule-null mutants of the low conjugating hypervirulent *K. pneumoniae* isolates (Appendix 2 Figure 11). However, the increases in conjugation frequency of pNDM1^{KmR} in $\Delta wcaJ$ suggests that capsule is not as much of a barrier to pKPC2 as it is to pNDM1.

Discussion

The spread of carbapenemase-encoding plasmids via horizontal gene transfer poses a major challenge to treatment against multidrug-resistant gram-negative bacteria because carbapenems are often antimicrobial agents of last resort. However, the dynamics and factors enabling the spread of these clinically significant plasmids have not been well studied. Previously, we found that pKPC2 is the only carbapenemase-encoding plasmid harbored by all the carbapenemase-resistant hypervirulent *K. pneumoniae* identified (5). Hypervirulent *K. pneumoniae* can cause *Klebsiella*-induced liver abscess, a community-acquired infection endemic in Asia-Pacific regions (29); the K1/ST23 lineage is predominantly responsible and causes 80% of these abscesses (30). Hypervirulent *K. pneumoniae* evolved through separate lineages from classical strains that typically cause multidrug-resistant nosocomial infections (30). Because hypervirulent *K. pneumoniae* is thought to be less receptive to horizontal gene transfer, pKPC2 in these strains could indicate that this plasmid has high transmission potential.

Our results showed that pKPC2 was the most prevalent carbapenemase-encoding plasmid among the clinical Enterobacterales isolates in CaPES. These plasmids are largely found in *K. pneumoniae*, *E. coli*, and *E. cloacae*, which also were the most prevalent carbapenemase-encoding plasmid-harboring species reported in other surveillance studies (31,32), showing that those are major reservoirs. Although KPC-2 has been documented on diverse plasmids and is known to undergo frequent recombination events (33), we uncovered a single plasmid that moves as a discrete and intact unit among diverse strains and species. One limitation of our epidemiologic study is

Table. Regression coefficients for pKPC2 and pNDM1 plasmid conjugation frequencies between donor-recipient pairs in a study of carbapenemase-encoding plasmids in clinical Enterobacteriales isolates and hypervirulent *Klebsiella pneumoniae*, Singapore*

Taxonomic relatedness (model parameter)	pKPC2		pNDM1	
	Mean	Bootstrap 95% CI	Mean	Bootstrap 95% CI
Same strain (β_0)	-1.73	-1.824 to -1.610	-2.31	-2.405 to -2.212
Same species (β_1)	-1.38	-1.599 to -1.147	-1.56	-1.771 to -1.317
Same genus (β_2)	-1.01	-1.162 to -0.866	-2.09	-2.258 to -1.907
Different genus (β_3)	0.04	-0.1165 to 0.1988	-1.94	-2.086 to -1.808

*log base 10 conjugation frequencies and their bootstrap 95% CI as described in for the regression equation and fitting procedure are shown.

that we do not yet know whether the same trend in plasmid transfer persisted after 2015.

Several factors revealed by our in vitro data potentially explain the high prevalence and dominance of pKPC2 in clinical isolates. First, pKPC2 conjugates with fast kinetics and has high transmissibility among various host-recipient pairs. Although taxonomic relatedness is known to affect conjugation frequency (21), pNDM1 is more strongly affected by this relatedness than pKPC2, especially for transfer within same and other genera. This finding likely accounts for the success of pKPC2 as the dominant carbapenemase-encoding plasmid among Enterobacteriales clinical isolates. Second, pKPC2 has low fitness costs and is highly adapted to host species. The persistence of plasmids in bacterial populations over an extended period has long been regarded as an evolutionary dilemma (34). Although compensatory mechanisms could account for plasmid persistence within a community with a high conjugation rate, offsetting the disadvantage incurred by high fitness cost in the absence of selection pressure (35), another study reported that the key factor for the persistence of the pOXA48_K8 plasmid is its low fitness costs across many clinical Enterobacteriaceae hosts in the gut, rather than its high conjugation frequency (36,37). We found that pKPC2 imposes low fitness cost and had high conjugation frequency across several Enterobacteriales isolates and a remarkable retention rate, even in low conjugating strains. pKPC2 exhibited no mutations after in vitro evolution experiments and almost no changes compared with original clinical isolates.

We noted that both the conjugative machinery and plasmid maintenance genes in pKPC2 are encoded by the pSA20021456.2-like backbone. Several plasmids with a similar backbone have been described (Figure 4, panel B), including the multidrug-resistant pHS102707 and the pJJ1886_4 plasmids found in clinical *E. coli* strains (38,39). This finding raises the concern that plasmids with this backbone might have similar dissemination potential or be able to recombine with plasmid fragments bearing multidrug-resistant genes and a suitable oriV to become dominant under antimicrobial drug selection pressure. Although we might never know the origins and the evolutionary

steps taken by pKPC2, one clue is its phylogenetic relatedness to IncP- ϵ plasmids, which have been observed to be vectors in the spread of antimicrobial drug resistance in agricultural systems (40).

The high transmissibility of pKPC2 was also seen in hypervirulent *K. pneumoniae* clinical isolates. Hypervirulent *K. pneumoniae* is thought to face constraints in horizontal gene transfer, and its low gene content diversity further supported the idea that the thick capsular polysaccharide is a barrier to transfer (41). Reports of $\Delta wcaJ$ in 4 different strains of *K. pneumoniae* showed an 8–20-fold increase in plasmid conjugation over 1 hour (42). Capsule deletion increased conjugation frequency by 10–100-fold in pNDM1 compared with pKPC2. This increase shows the capsule is more of a hindrance to pNDM1 than to pKPC2, suggesting that pKPC2 has a competitive advantage over pNDM1 in its transmission to encapsulated strains. This finding might explain why pKPC2 is the only carbapenemase-encoding plasmid among all the hypervirulent/carbapenem-resistant *K. pneumoniae* isolates we discovered (5). The high transmissibility of pKPC2 to the antimicrobial-sensitive, community-acquired hypervirulent *K. pneumoniae* strains suggests that pKPC2 or its predecessors might have undergone carriage selection for high transmissibility and persistence in isolates from ecologic settings that harbor similar features to hypervirulent *K. pneumoniae*. Although our mechanistic studies of plasmid transmission are limited to in vitro experiments, these studies provide insights and potential explanations on the pattern of transmission observed clinically.

In summary, this study underscores the need to track the spread and dominance of clinically relevant carbapenemase-encoding plasmids in health-care settings and examine transmission characteristics. Our findings reveal increasing dominance of pKPC2 over other carbapenemase-encoding plasmids during a 5-year period. pKPC2 appears to be a highly adapted hybrid plasmid exhibiting increased transmissibility and persistence among Enterobacteriales and hypervirulent *K. pneumoniae* strains. These highly evolved and adapted plasmids act as agents that move easily between various hosts and exert negligible fitness costs, facilitating their long-

term carriage even without selection pressure. We propose that the pKPC2 plasmid has already undergone carriage adaptation and been in circulation for some time. Insights gained on the transmission potential of pKPC2 and other similarly evolved plasmids could translate into better infection prevention measures or improved surveillance.

Acknowledgments

We thank Swaine Chen for the gift of bacterial strains. We also thank the CaPES study group for their support; this group included Benjamin Cherng, Deepak Rama Narayana, Douglas Chan Su Gin, De Partha Pratim, Hsu Li Yang, Indumathi Venkatachalam, Jeanette Teo, Michelle Ang, Kalisvar Marimuthu, Koh Tse Hsien, Nancy Tee, Nares Smitasin, Ng Oon Tek, Ooi Say Tat, Raymond Fong, Raymond Lin Tzer Pin, Surinder Kaur Pada, Tan Thean Yen, and Thoon Koh Cheng.

N.M.T., P.S.R.S., K.M., V. K., and O.T.N. were supported by the Singapore Ministry of Health's National Medical Research Council (NMRC) under its collaborative grants, including Collaborative Solutions Targeting Antimicrobial Resistance Threats in Health Systems (CoSTAR-HS) (grant no. NMRC CGAug16C005), NMRC Clinician Scientist Award (grant no. MOH-000276), and NMRC Clinician Scientist Individual Research Grant (no. MOH-CIRG18nov-0006); the National Centre for Infectious Diseases under its NCID Catalyst Grant (no. FY202013VKHQ); and the German Federal Ministry of Health COVID-19 research and development funding to the World Health Organization (award no. 70826). A.E.M. was supported by Grant FONDECYT (no. 11181135), from Agencia Nacional de Investigación y Desarrollo, Chile. This research was also supported by NMRC grant nos. OFIRG20NOV-0045 and MOE2018-T3-1-03 to Y.H.G.

About the Author

Mr. Yong is a doctoral student at the Department of Biochemistry, Infectious Diseases Translational Research Program, Yong Loo Lin School of Medicine, National University of Singapore. His main research interest is plasmid transmission and the development of novel antimicrobial drugs.

References

- World Health Organization. Global priority list of antibiotic-resistant bacteria to guide research, discovery, and development of new antibiotics. Geneva: The Organization; 2017.
- Yang X, Dong N, Chan EW, Zhang R, Chen S. Carbapenem resistance-encoding and virulence-encoding conjugative plasmids in *Klebsiella pneumoniae*. Trends Microbiol. 2021;29:65–83. <https://doi.org/10.1016/j.tim.2020.04.012>
- Benz F, Huisman JS, Bakkeren E, Herter JA, Stadler T, Ackermann M, et al. Plasmid- and strain-specific factors drive variation in ESBL-plasmid spread in vitro and in vivo. ISME J. 2021;15:862–78. <https://doi.org/10.1038/s41396-020-00819-4>
- Rodríguez-Beltrán J, DelaFuente J, León-Sampedro R, MacLean RC, San Millán Á. Beyond horizontal gene transfer: the role of plasmids in bacterial evolution. Nat Rev Microbiol. 2021;19:347–59. <https://doi.org/10.1038/s41579-020-00497-1>
- Chen Y, Marimuthu K, Teo J, Venkatachalam I, Cherng BPZ, De Wang L, et al. Acquisition of plasmid with carbapenem-resistance gene *bla*_{KPC2} in hypervirulent *Klebsiella pneumoniae*, Singapore. Emerg Infect Dis. 2020;26:549–59. <https://doi.org/10.3201/eid2603.191230>
- Marimuthu K, Venkatachalam I, Khong WX, Koh TH, Cherng BPZ, Van La M, et al.; Carbapenemase-Producing Enterobacteriaceae in Singapore (CaPES) Study Group. Clinical and molecular epidemiology of carbapenem-resistant Enterobacteriaceae among adult inpatients in Singapore. Clin Infect Dis. 2017;64:S68–75. <https://doi.org/10.1093/cid/cix113>
- Bankovich A, Nurk S, Antipov D, Gurevich AA, Dvorkin M, Kulikov AS, et al. SPAdes: a new genome assembly algorithm and its applications to single-cell sequencing. J Comput Biol. 2012;19:455–77. <https://doi.org/10.1089/cmb.2012.0021>
- Wick RR, Judd LM, Gorrie CL, Holt KE. Unicycler: resolving bacterial genome assemblies from short and long sequencing reads. PLOS Comput Biol. 2017;13:e1005595. <https://doi.org/10.1371/journal.pcbi.1005595>
- Jolley KA, Maiden MC. BIGSdb: Scalable analysis of bacterial genome variation at the population level. BMC Bioinformatics. 2010;11:595. <https://doi.org/10.1186/1471-2105-11-595>
- Wood DE, Salzberg SL. Kraken: ultrafast metagenomic sequence classification using exact alignments. Genome Biol. 2014;15:R46. <https://doi.org/10.1186/gb-2014-15-3-r46>
- Seemann T. Abricate [cited 2021 Aug 5]. <https://github.com/tseemann/abricate>
- Feldgarden M, Brover V, Haft DH, Prasad AB, Slotta DJ, Tolstoy I, et al. Validating the AMRFinder tool and resistance gene database by using antimicrobial resistance genotype-phenotype correlations in a collection of isolates. Antimicrob Agents Chemother. 2019;63:e00483-19. <https://doi.org/10.1128/AAC.00483-19>
- Chen L, Zheng D, Liu B, Yang J, Jin Q. VFDB 2016: hierarchical and refined dataset for big data analysis – 10 years on. Nucleic Acids Res. 2016;44:D694–7. <https://doi.org/10.1093/nar/gkv1239>
- Besemer J, Lomsadze A, Borodovsky M. GeneMarkS: a self-training method for prediction of gene starts in microbial genomes. Implications for finding sequence motifs in regulatory regions. Nucleic Acids Res. 2001;29:2607–18. <https://doi.org/10.1093/nar/29.12.2607>
- Alikhan NF, Petty NK, Ben Zakour NL, Beatson SA. BLAST Ring Image Generator (BRIG): simple prokaryote genome comparisons. BMC Genomics. 2011;12:402. <https://doi.org/10.1186/1471-2164-12-402>
- Carattoli A, Zankari E, García-Fernández A, Voldby Larsen M, Lund O, Villa L, et al. In silico detection and typing of plasmids using PlasmidFinder and plasmid multilocus sequence typing. Antimicrob Agents Chemother. 2014;58:3895–903. <https://doi.org/10.1128/AAC.02412-14>
- Robertson J, Nash JHE. MOB-suite: software tools for clustering, reconstruction and typing of plasmids from draft assemblies. Microb Genom. 2018;4. <https://doi.org/10.1099/mgen.0.000206>

18. Kumar S, Stecher G, Li M, Knyaz C, Tamura K. MEGA X: Molecular Evolutionary Genetics Analysis across computing platforms. *Mol Biol Evol.* 2018;35:1547–9. <https://doi.org/10.1093/molbev/msy096>
19. De Gelder L, Ponciano JM, Joyce P, Top EM. Stability of a promiscuous plasmid in different hosts: no guarantee for a long-term relationship. *Microbiology (Reading).* 2007;153:452–63. <https://doi.org/10.1099/mic.0.2006/001784-0>
20. Cook TB, Rand JM, Nurani W, Courtney DK, Liu SA, Pfeiffer BF. Genetic tools for reliable gene expression and recombineering in *Pseudomonas putida*. *J Ind Microbiol Biotechnol.* 2018;45:517–27. <https://doi.org/10.1007/s10295-017-2001-5>
21. Alderliesten JB, Duxbury SJN, Zwart MP, de Visser JAGM, Stegeman A, Fischer EAJ. Effect of donor-recipient relatedness on the plasmid conjugation frequency: a meta-analysis. *BMC Microbiol.* 2020;20:135. <https://doi.org/10.1186/s12866-020-01825-4>
22. Ageevets V, Sopova J, Lazareva I, Malakhova M, Ilina E, Kostryukova E, et al. Genetic environment of the *bla*_{KPC-2} Gene in a *Klebsiella pneumoniae* isolate that may have been imported to Russia from Southeast Asia. *Antimicrob Agents Chemother.* 2017;61:e01856-16. <https://doi.org/10.1128/AAC.01856-16>
23. Miki T, Easton AM, Rownd RH. Cloning of replication, incompatibility, and stability functions of R plasmid NRI. *J Bacteriol.* 1980;141:87–99. <https://doi.org/10.1128/jb.141.1.87-99.1980>
24. Lovett MA, Helinski DR. Method for the isolation of the replication region of a bacterial replicon: construction of a mini-F⁺ plasmid. *J Bacteriol.* 1976;127:982–7. <https://doi.org/10.1128/jb.127.2.982-987.1976>
25. Thomas CM, Smith CA. Incompatibility group P plasmids: genetics, evolution, and use in genetic manipulation. *Annu Rev Microbiol.* 1987;41:77–101. <https://doi.org/10.1146/annurev.mi.41.100187.000453>
26. Novick RP. Plasmid incompatibility. *Microbiol Rev.* 1987;51:381–95. <https://doi.org/10.1128/mr.51.4.381-395.1987>
27. Pansegrau W, Lanka E, Barth PT, Figurski DH, Guiney DG, Haas D, et al. Complete nucleotide sequence of Birmingham IncP alpha plasmids. Compilation and comparative analysis. *J Mol Biol.* 1994;239:623–63. <https://doi.org/10.1006/jmbi.1994.1404>
28. Stalder T, Rogers LM, Renfrow C, Yano H, Smith Z, Top EM. Emerging patterns of plasmid-host coevolution that stabilize antibiotic resistance. *Sci Rep.* 2017;7:4853. <https://doi.org/10.1038/s41598-017-04662-0>
29. Lee CR, Lee JH, Park KS, Jeon JH, Kim YB, Cha CJ, et al. Antimicrobial resistance of hypervirulent *Klebsiella pneumoniae*: epidemiology, hypervirulence-associated determinants, and resistance mechanisms. *Front Cell Infect Microbiol.* 2017;7:483. <https://doi.org/10.3389/fcimb.2017.00483>
30. Lam MMC, Wyres KL, Duchêne S, Wick RR, Judd LM, Gan YH, et al. Population genomics of hypervirulent *Klebsiella pneumoniae* clonal-group 23 reveals early emergence and rapid global dissemination. *Nat Commun.* 2018;9:2703. <https://doi.org/10.1038/s41467-018-05114-7>
31. Sugawara Y, Hagiya H, Akeda Y, Aye MM, Myo Win HP, Sakamoto N, et al. Dissemination of carbapenemase-producing Enterobacteriaceae harbouring *bla*_{NDM} or *bla*_{IMI} in local market foods of Yangon, Myanmar. *Sci Rep.* 2019;9:14455. <https://doi.org/10.1038/s41598-019-51002-5>
32. Miltgen G, Cholley P, Martak D, Thouverez M, Seraphin P, Leclaire A, et al. Carbapenemase-producing Enterobacteriaceae circulating in the Reunion Island, a French territory in the Southwest Indian Ocean. *Antimicrob Resist Infect Control.* 2020;9:36. <https://doi.org/10.1186/s13756-020-0703-3>
33. David S, Cohen V, Reuter S, Sheppard AE, Giani T, Parkhill J, et al.; European Survey of Carbapenemase-Producing Enterobacteriaceae (EuSCAPE) Working Group; ESCMID Study Group for Epidemiological Markers (ESGEM). Integrated chromosomal and plasmid sequence analyses reveal diverse modes of carbapenemase gene spread among *Klebsiella pneumoniae*. *Proc Natl Acad Sci U S A.* 2020;117:25043–54. <https://doi.org/10.1073/pnas.2003407117>
34. Harrison E, Brockhurst MA. Plasmid-mediated horizontal gene transfer is a coevolutionary process. *Trends Microbiol.* 2012;20:262–7. <https://doi.org/10.1016/j.tim.2012.04.003>
35. Lopatkin AJ, Meredith HR, Srimani JK, Pfeiffer C, Durrett R, You L. Persistence and reversal of plasmid-mediated antibiotic resistance. *Nat Commun.* 2017;8:1689. <https://doi.org/10.1038/s41467-017-01532-1>
36. Alonso-del Valle A, León-Sampedro R, Rodríguez-Beltrán J, DelaFuente J, Hernández-García M, Ruiz-Garbayosa P, et al. Viability of plasmid fitness effects contributes to plasmid persistence in bacterial communities. *Nat Commun.* 2021;12:2653. <https://doi.org/10.1038/s41467-021-22849-y>
37. León-Sampedro R, DelaFuente J, Díaz-Agero C, Crellen T, Musicha P, Rodríguez-Beltrán J, et al.; R-GNOSIS WP5 Study Group. Pervasive transmission of a carbapenem resistance plasmid in the gut microbiota of hospitalized patients. *Nat Microbiol.* 2021;6:606–16. <https://doi.org/10.1038/s41564-021-00879-y>
38. Li G, Zhang Y, Bi D, Shen P, Ai F, Liu H, et al. First report of a clinical, multidrug-resistant *Enterobacteriaceae* isolate coharboring fosfomycin resistance gene *fosA3* and carbapenemase gene *bla*_{KPC-2} on the same transposon, Tn1721. *Antimicrob Agents Chemother.* 2015;59:338–43. <https://doi.org/10.1128/AAC.03061-14>
39. Andersen PS, Stegger M, Aziz M, Contente-Cuomo T, Gibbons HS, Keim P, et al. Complete genome sequence of the epidemic and highly virulent CTX-M-15-producing H30-Rx subclone of *Escherichia coli* ST131. *Genome Announc.* 2013;1:e00988-13. <https://doi.org/10.1128/genomeA.00988-13>
40. Heuer H, Binh CT, Jechalke S, Kopmann C, Zimmerling U, Krögerrecklenfort E, et al. IncP-1ε plasmids are important vectors of antibiotic resistance genes in agricultural systems: diversification driven by class 1 integron gene cassettes. *Front Microbiol.* 2012;3:2. <https://doi.org/10.3389/fmicb.2012.00002>
41. Wyres KL, Wick RR, Judd LM, Froumine R, Tokolyi A, Gorrie CL, et al. Distinct evolutionary dynamics of horizontal gene transfer in drug resistant and virulent clones of *Klebsiella pneumoniae*. *PLoS Genet.* 2019;15:e1008114. <https://doi.org/10.1371/journal.pgen.1008114>
42. Haudiquet M, Buffet A, Rendueles O, Rocha EPC. Interplay between the cell envelope and mobile genetic elements shapes gene flow in populations of the nosocomial pathogen *Klebsiella pneumoniae*. *PLoS Biol.* 2021;19:e3001276. <https://doi.org/10.1371/journal.pbio.3001276>

Address for correspondence: Yunn-Hwen Gan, Infectious Diseases Translational Research Program, National University Singapore Yong Loo Lin School of Medicine, Biochemistry MD7, 8 Medical Dr, Singapore 117596, Singapore; email: bchganyh@nus.edu.sg

Dominant Carbapenemase-Encoding Plasmids in Clinical Enterobacterales Isolates and Hypervirulent *Klebsiella pneumoniae*, Singapore

Appendix 2

Supplementary Methods

Mutant Generation

To delete genes/regions in hypervirulent *Klebsiella pneumoniae*, ≈1,000-bp fragments upstream and downstream of the target were amplified with PCR (Appendix 2 Table 3) from genomic DNA templates with Taq polymerase and then assembled in a conditional suicide pR6KmobSacB vector by using NEBuilder HiFi DNA Assembly Master Mix (New England Biolabs). The vectors were then transformed into *Escherichia coli* S17-1 λ pir competent cells before being conjugated into hypervirulent *K. pneumoniae* strains. Single crossover transconjugants were selected on lysogeny agar with kanamycin + fosfomycin (50 μ g/mL + 40 μ g/mL) and subcultured in lysogeny broth containing 15% sucrose without NaCl. Kanamycin-sensitive, double crossovers were screened for successful deletion by PCR. For the generation of capsule null mutants in NUH66, TTSH25, and SGH07, genomes were first annotated with Prokka 1.13 (1) to locate the initial glycotransferase *wcaJ* gene. The *wcaJ* gene was deleted in each strain by using the same method.

Construction of Plasmids

Plasmids were introduced into bacterial strains by electroporation, chemical transformation, or conjugation (Appendix 2 Table 2). Plasmids were constructed by first amplifying individual fragments from various plasmids by using Q5 High-Fidelity DNA Polymerase (New England Biolabs, NEB) in PCR and then all the fragments were assembled by using NEBuilder HiFi DNA Assembly Cloning Kit (NEB). Plasmid mutants were generated

based on the Lambda Red system (2) with some modifications. First, a curable Lambda Red plasmid (pACYC-flp-Red-sacB) was generated by combining the enhanced Flp recombinase gene from pFLPe2 (3), the Lambda Red recombinase genes from pKD46 (4), and the *sacB* gene from pK18mobsacB (5) into pACYC184 (6). Electroporation-competent cells of *E. coli* MG1655 carrying pACYC-flp-Red-sacB and pKPC2 or pNDM1 were prepared in the presence of L-arabinose (0.2%). The competent cells were electroporated with PCR product of chloramphenicol resistance gene (CmR) or kanamycin resistance gene (KmR) with 40-nt extensions that are homologous to regions adjacent to the gene to be inactivated. CmR or KmR transformants were selected. Gene replacement was verified by colony PCR. The pACYC-flp-Red-sacB plasmid was cured from the strain by growing them in medium containing sucrose (15%).

Plasmid Genome Sequence Reference Database

Reference plasmid genome sequences for each carbapenemase gene allele were derived from 2 sources: NCBI RefSeq database (<https://www.ncbi.nlm.nih.gov/refseq>) or fully circularized plasmid genome sequences from hybrid assemblies based on Oxford Nanopore Technologies (ONT, <https://nanoporetech.com>). Complete plasmid sequences were downloaded from NCBI RefSeq database by using the search term “plasmid.” The downloaded sequence data were further filtered to only include plasmid sequences with identifiers that met the keyword criteria “plasmid” AND “circular” NOT “gene” NOT “partial” NOT “incomplete” NOT “putative.” Additionally, the dataset was filtered to remove exact duplicate sequences. All known alleles from ARG-ANNOT database (7) were downloaded and plasmid sequences were aligned against the carbapenemase gene allele sequences. Only plasmids that had 100% coverage and 100% identity with the carbapenemase gene allele were incorporated into the database (n = 396). Second, a set of fully circularized plasmid genome sequences (n = 542) extracted from ONT-based hybrid assemblies were added to the reference database using the same criteria for the specific carbapenemase gene allele presence. In total, the plasmid genome sequence reference database contained 938 complete plasmid sequences. Subsequently, a self-BLAST was performed and sequences that shared 99% identity, 99% query coverage, and 99% subject coverage were grouped into clusters.

Identification of Carbapenemase-Encoding Plasmids for Each Isolate

For each isolate, fully circularized CP sequence was identified from among the 542 hybrid assemblies described above, if available. For isolates that did not have a fully circularized carbapenemase-encoding plasmids sequence, plasmid identification was performed using the following steps: (i) PlasmidSeeker (v0.1; 2017–04–21) was run using the Illumina reads as input and with default parameters against the carbapenemase gene allele-specific reference database described above ($n = 938$) to obtain candidate plasmids; (ii) For each isolate, the carbapenemase gene-containing contig (carrying the carbapenemase gene with at least 99% identity and 90% gene coverage) was identified from the Illumina assembly; (iii) The carbapenemase gene-containing contig identified in step (ii) was aligned using the NCBI BLAST tool against the candidate plasmids obtained by PlasmidSeeker in step (i), only retaining candidate plasmids sharing $\geq 90\%$ k-mers with the isolate as determined by PlasmidSeeker, and carbapenemase gene-containing contig BLAST alignment coverage of $\geq 90\%$; (iv) Finally, the specific CP-plasmid for each isolate was determined according to the following selection criteria consecutively: highest query coverage, highest k-mer coverage, and longest plasmid. For isolates that still had multiple valid candidate plasmid assignments, priority was given to the dominant plasmid that was determined for the given carbapenemase gene. Cluster assignment was derived from the cluster membership of the assigned carbapenemase-encoding plasmid. The largest cluster of carbapenemase-encoding plasmids for a given carbapenemase gene was termed as the dominant cluster.

Survival-Analysis Approach

We used the dataset shown in Appendix 2 Figures 8 and 9 comprising 98 donor-recipient pairs, we first classified each pair into one of 4 levels of taxonomic relatedness: same strain, same species, same genus, or different genera. The full dataset of log-conjugation frequencies for pKPC2 (522 datapoints) or pNDM1 (530 datapoints) was regressed against this variable. Unobserved plasmid conjugation events were taken to be left-censored, with the detection limit set at $1e-8$ (as the minimum observed value was $5e-8$). Donor-recipient pair was modeled as a random effect to account for unobserved heterogeneity specific to each pair (such as incompatible plasmids in the recipient).

Mathematically,

$$\log_{10} f = \beta_0 + \beta_1(\text{same species}) + \beta_2(\text{same genus}) + \beta_3(\text{other genus}),$$

where f is the conjugation frequency, β_0 is the baseline log-conjugation frequency between the same strain, and β_1 , β_2 , and β_3 denote the relative change in log-conjugation frequency for transfer between the same species, same genus, or other genus, respectively. The coefficients β_0 , β_1 , β_2 , and β_3 were inferred using the `survreg` function of the R survival package (version 3.1-12) (8), with donor-recipient pair modeled as a gaussian frailty. The 95% confidence intervals were computed from 1,000 bootstrap replicates using the R `boot` package version 1.3-28 (9).

Data Availability

Raw sequence data from this study were uploaded to the NCBI Sequence Read Archive (SRA) Database under Bioproject accession numbers PRJNA757551 and PRJNA765801 for the Illumina short-read sequencing data, PRJNA801425 for the Oxford Nanopore Technologies (ONT) long-read sequencing data for the plasmid growth rate experiment, and PRJNA801415 for the ONT long-read sequencing data that contributed to the plasmid genome reference sequence database.

References

1. Seemann T. Prokka: rapid prokaryotic genome annotation. *Bioinformatics*. 2014;30:2068–9. PubMed <https://doi.org/10.1093/bioinformatics/btu153>
2. Murphy KC. Use of bacteriophage lambda recombination functions to promote gene replacement in *Escherichia coli*. *J Bacteriol*. 1998;180:2063–71. PubMed <https://doi.org/10.1128/JB.180.8.2063-2071.1998>
3. Choi KH, Mima T, Casart Y, Rholl D, Kumar A, Beacham IR, et al. Genetic tools for select-agent-compliant manipulation of *Burkholderia pseudomallei*. *Appl Environ Microbiol*. 2008;74:1064–75. PubMed <https://doi.org/10.1128/AEM.02430-07>
4. Datsenko KA, Wanner BL. One-step inactivation of chromosomal genes in *Escherichia coli* K-12 using PCR products. *Proc Natl Acad Sci U S A*. 2000;97:6640–5. PubMed <https://doi.org/10.1073/pnas.120163297>
5. Kvitko BH, Collmer A. Construction of *Pseudomonas syringae* pv. tomato DC3000 mutant and polymutant strains. *Methods Mol Biol*. 2011;712:109–28. PubMed https://doi.org/10.1007/978-1-61737-998-7_10

6. Chang AC, Cohen SN. Construction and characterization of amplifiable multicopy DNA cloning vehicles derived from the P15A cryptic miniplasmid. *J Bacteriol.* 1978;134:1141–56. PubMed <https://doi.org/10.1128/jb.134.3.1141-1156.1978>
7. Gupta SK, Padmanabhan BR, Diene SM, Lopez-Rojas R, Kempf M, Landraud L, et al. ARG-ANNOT, a new bioinformatic tool to discover antibiotic resistance genes in bacterial genomes. *Antimicrob Agents Chemother.* 2014;58:212–20. PubMed <https://doi.org/10.1128/AAC.01310-13>
8. Therneau T. A package for survival analysis in R [cited 2021 Aug 5]. <https://github.com/therneau/survival>
9. Canty A, Ripley BD. boot: Bootstrap R (S-Plus) functions [cited 2021 Aug 5]. <https://cran.r-project.org/web/packages/boot/index.html>
10. Blattner FR, Plunkett G III, Bloch CA, Perna NT, Burland V, Riley M, et al. The complete genome sequence of *Escherichia coli* K-12. *Science.* 1997;277:1453–62. PubMed <https://doi.org/10.1126/science.277.5331.1453>
11. Khetrpal V, Mehershahi K, Rafee S, Chen S, Lim CL, Chen SL. A set of powerful negative selection systems for unmodified *Enterobacteriaceae*. *Nucleic Acids Res.* 2015;43:e83. PubMed <https://doi.org/10.1093/nar/gkv248>
12. Mulvey MA, Schilling JD, Hultgren SJ. Establishment of a persistent *Escherichia coli* reservoir during the acute phase of a bladder infection. *Infect Immun.* 2001;69:4572–9. PubMed <https://doi.org/10.1128/IAI.69.7.4572-4579.2001>
13. Massip C, Branchu P, Bossuet-Greif N, Chagneau CV, Gaillard D, Martin P, et al. Deciphering the interplay between the genotoxic and probiotic activities of *Escherichia coli* Nissle 1917. *PLoS Pathog.* 2019;15:e1008029. PubMed <https://doi.org/10.1371/journal.ppat.1008029>
14. de Lorenzo V, Cases I, Herrero M, Timmis KN. Early and late responses of TOL promoters to pathway inducers: identification of postexponential promoters in *Pseudomonas putida* with lacZ-tet bicistronic reporters. *J Bacteriol.* 1993;175:6902–7. PubMed <https://doi.org/10.1128/jb.175.21.6902-6907.1993>
15. Lee IR, Molton JS, Wyres KL, Gorrie C, Wong J, Hoh CH, et al. Differential host susceptibility and bacterial virulence factors driving *Klebsiella* liver abscess in an ethnically diverse population. *Sci Rep.* 2016;6:29316. PubMed <https://doi.org/10.1038/srep29316>

16. Lee KW, Arumugam K, Purbojati RW, Tay QX, Williams RB, Kjelleberg S, et al. Draft genome sequence of *Klebsiella pneumoniae* strain KP-1. *Genome Announc.* 2013;1:e01082-13. PubMed <https://doi.org/10.1128/genomeA.01082-13>
17. Lam MMC, Wyres KL, Duchêne S, Wick RR, Judd LM, Gan YH, et al. Population genomics of hypervirulent *Klebsiella pneumoniae* clonal-group 23 reveals early emergence and rapid global dissemination. *Nat Commun.* 2018;9:2703. PubMed <https://doi.org/10.1038/s41467-018-05114-7>
18. Tan YH, Chen Y, Chu WHW, Sham LT, Gan YH. Cell envelope defects of different capsule-null mutants in K1 hypervirulent *Klebsiella pneumoniae* can affect bacterial pathogenesis. *Mol Microbiol.* 2020;113:889–905. PubMed <https://doi.org/10.1111/mmi.14447>
19. Chen Y, Marimuthu K, Teo J, Venkatachalam I, Cherng BPZ, De Wang L, et al. Acquisition of plasmid with carbapenem-resistance gene *bla_{KPC2}* in hypervirulent *Klebsiella pneumoniae*, Singapore. *Emerg Infect Dis.* 2020;26:549–59. PubMed <https://doi.org/10.3201/eid2603.191230>
20. Cook TB, Rand JM, Nurani W, Courtney DK, Liu SA, Pflieger BF. Genetic tools for reliable gene expression and recombineering in *Pseudomonas putida*. *J Ind Microbiol Biotechnol.* 2018;45:517–27. PubMed <https://doi.org/10.1007/s10295-017-2001-5>

Appendix 2 Table 1. Description of *Enterobacteriales* strains used for carbapenemase-encoding plasmids in clinical isolates and hypervirulent *Klebsiella pneumoniae*, Singapore*

Strains	Features	Virulence factors	Source or reference
<i>Enterobacter cloacae</i> ATCC 13047	Type strain	ND	ATCC
<i>Escherichia coli</i> MG1655	K-12	ND	(10)
SLC-568	MG1655 <i>hdsS</i> :kan	ND	(11)
UTI89	Uropathogenic strain	ND	(12)
Nissle 1917	Probiotic strain	ND	(13)
S17-1 λ pir	Conjugation donor carrying an integrated RP4-2 and λ pir, TpR	ND	(14)
<i>Enterobacter hormaechei</i> ATCC 700323	Quality control strain	ND	ATCC
<i>Klebsiella quasipneumoniae</i> TTSH04	KL114, ST2037	ND	(15)
<i>K. oxytoca</i> 8071169380	Clinical isolate	ND	This study
8071167205	Clinical isolate	ND	This study
<i>K. variicola</i> NUH59	KL10, ST906	ND	This study
<i>K. pneumoniae</i> ATCC 13883	KL3, ST3, type strain	ND	ATCC
NUH29	KL28, ST20	ND	(15)
KP-1	KL54, ST29, environmental isolate	ND	(16)
NUH03	KL2, ST65	ICEKp10, <i>iuc</i> , <i>clb</i> , <i>iro</i> , <i>rmpA</i>	(15)
NUH04	KL2, ST2039	ICEKp10, <i>iuc</i> , <i>clb</i> , <i>iro</i> , <i>rmpA</i>	(15)
NUH06	KL1, ST23	ICEKp3, <i>iuc</i> , <i>iro</i> , <i>rmpA</i>	(15)
NUH13	KL1, ST2044	ICEKp10, <i>iuc</i> , <i>clb</i> , <i>iro</i> , <i>rmpA</i>	(15)
NUH14	KL2, ST380	<i>iuc</i> , <i>clb</i> , <i>iro</i> , <i>rmpA</i>	(15)
NUH26	KL5, ST1049	ICEKp6, <i>iuc</i> , <i>iro</i> , <i>rmpA</i>	(15)
NUH40	KL5, ST1049	ICEKp6, <i>iuc</i> , <i>iro</i> , <i>rmpA</i>	This study
NUH61	KL2, ST86	<i>iuc</i> , <i>iro</i> , <i>rmpA</i>	This study
NUH66	KL2, ST2039	ICEKp10, <i>iuc</i> , <i>clb</i> , <i>iro</i> , <i>rmpA</i>	This study
NUH66 Δ <i>wcaJ</i>	NUH66, <i>wcaJ</i> deletion (capsule null; deletion of initial glycosyltransferase)	<i>iuc</i> , <i>clb</i> , <i>iro</i> , <i>rmpA</i>	This study
SGH07	KL5, ST60	ICEKp1, <i>iro</i> , <i>rmpA</i>	(15)
SGH07 Δ <i>wcaJ</i>	SGH07, <i>wcaJ</i> deletion	<i>iro</i> , <i>rmpA</i>	This study
TTSH21	KL5, ST60	ICEKp1, <i>iro</i> , <i>rmpA</i>	This study
TTSH25	KL2, ST2039	ICEKp10, <i>iuc</i> , <i>clb</i> , <i>iro</i> , <i>rmpA</i>	(15)
TTSH25 Δ <i>wcaJ</i>	TTSH25, <i>wcaJ</i> deletion (capsule null; deletion of initial glycosyltransferase)	<i>iuc</i> , <i>clb</i> , <i>iro</i> , <i>rmpA</i>	This study
SGH10	KL1, ST23	ICEKp10, <i>iuc</i> , <i>clb</i> , <i>iro</i> , <i>rmpA</i>	(17)
SGH10 Δ <i>wcaJ</i>	SGH10, <i>wcaJ</i> deletion (capsule null; deletion of initial glycosyltransferase)	ICEKp10, <i>iuc</i> , <i>clb</i> , <i>iro</i> , <i>rmpA</i>	(18)
SGH10 Δ <i>rmpA</i>	SGH10, <i>rmpA</i> deletion (deletion of <i>rmpA</i> abrogates the hypermucoviscous phenotype)	ICEKp10, <i>iuc</i> , <i>clb</i> , <i>iro</i>	(19)
SGH10 Δ GIE492	SGH10, GIE492 deletion (deletion of genomic island responsible for the production of microcin E492 and salmochelin)	ICEKp10, <i>iuc</i> , <i>clb</i> , <i>rmpA</i>	This study
SGH10 Δ T6SS1 Δ T6SS3	SGH10, T6SS1 and T6SS3 deletion (deletion of the two clusters of type 6 secretion system)	ICEKp10, <i>iuc</i> , <i>clb</i> , <i>iro</i> , <i>rmpA</i>	This study
SGH10 Δ ICEKp10	SGH10, ICEKp10 deletion (deletion of the chromosomal integrative and conjugative element encoding colibactin and yersiniabactin)	<i>iuc</i> , <i>iro</i> , <i>rmpA</i>	This study
SGH10 Δ <i>mrkA</i>	SGH10, <i>mrkA</i> deletion (deletion of the gene encoded for major subunit of type 3 fimbriae)	ICEKp10, <i>iuc</i> , <i>clb</i> , <i>iro</i> , <i>rmpA</i>	This study
SGH10 Δ KpVP	SGH10, KpVP deletion	ICEKp10, <i>clb</i>	This study
SGH10 Δ <i>mrkA</i> Δ KpVP	SGH10, KpVP and <i>mrkA</i> deletion	ICEKp10, <i>clb</i>	This study

*ATCC, American Type Culture Collection (<https://www.atcc.org>); ND, not done.

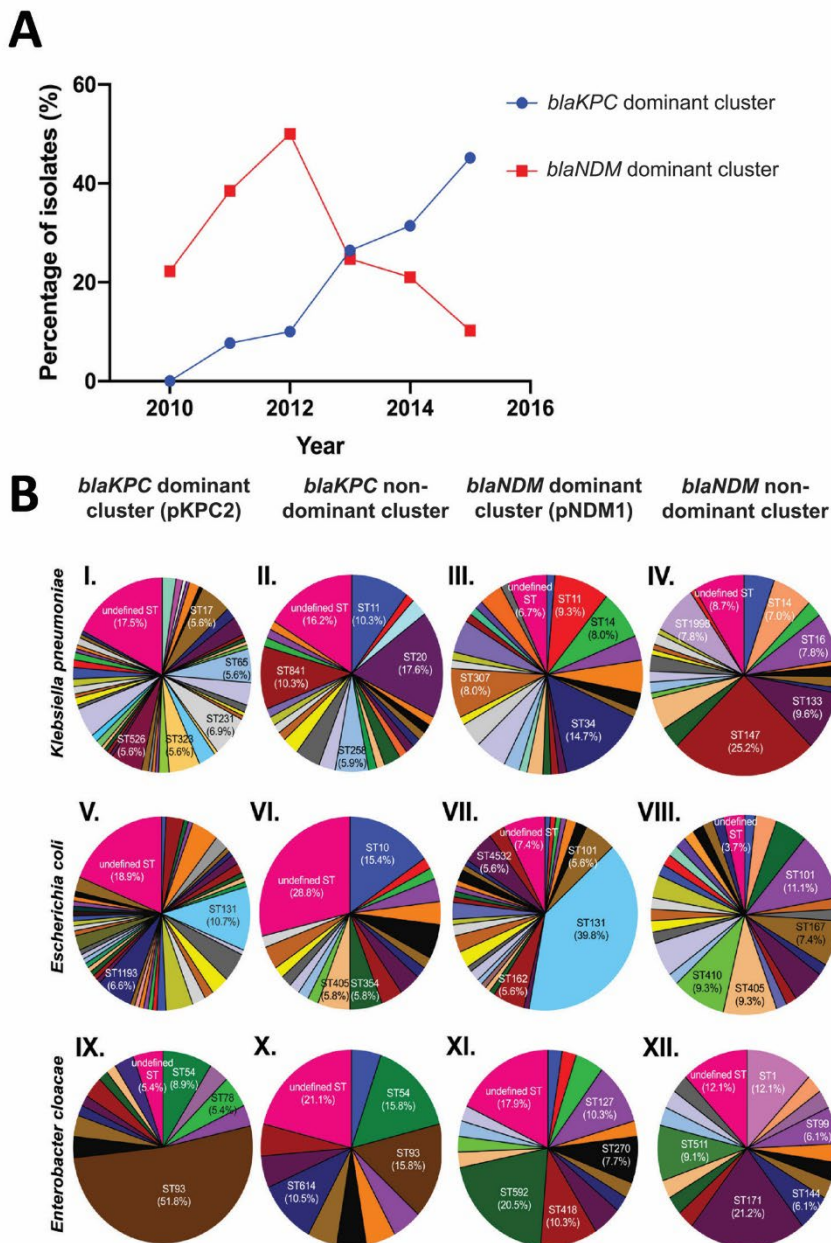
Appendix 2 Table 2. Description of carbapenemase-encoding plasmids used in a study of clinical *Enterobacteriales* isolates and hypervirulent *Klebsiella pneumoniae*, Singapore

Plasmid	Features	Source
pACYC184	Low copy number plasmid with a p15A replicon, CmR, TcR	(6)
pFLPe2	Source of zeocin resistance gene and Flp recombinase gene driven by PrhaB promoter, ZnR	(3)
pK18mobsacB	Source of sucrose counter-selection gene <i>sacB</i> , KmR	(5)
pR6KmobsacB	Conditional replicative plasmid carrying <i>sacB</i> and oriT, KmR	(18)
pKD46	Source of Red recombinases driven by Pbad promoter, ApR	(4)
pACYC-flp-Red-sacB	A p15A plasmid carrying <i>Flp</i> gene, Lambda Red recombinase genes and <i>sacB</i> gene, TcR	This study
pKD3	Source of chloramphenicol resistance gene flanked by FRT sites (FRT-Cm), CmR	(4)
pKD4	Source of kanamycin resistance gene flanked by FRT sites (FRT-Km), KmR	(4)
pKPC2	Conjugative plasmid from ENT494 carrying a <i>bla</i> _{KPC-2} gene, CbR	(19)
pKPC2 ^{KmR}	pKPC2 containing a kanamycin resistance gene from pKD4, CbR, KmR	This study
pKPC2 ^{KmR} Δ <i>higB</i>	pKPC2, <i>higB</i> was replaced with a kanamycin resistance gene, KmR	This study
pKPC2 Δ <i>parB</i>	pKPC2, <i>parB</i> was replaced with a chloramphenicol resistance gene, CmR	This study
pNDM1	Conjugative plasmid from ENT448 carrying a <i>bla</i> _{NDM-1} gene, CbR	This study
pNDM1 ^{KmR}	pNDM1 containing a kanamycin resistance gene from pKD4, CbR, KmR	This study
pRK2-AraE	IncP plasmid encoding <i>trfA</i> replication protein	(20)

Appendix 2 Table 3. Primers used in mutant generation for carbapenemase-encoding plasmids in clinical *Enterobacteriales* isolates and hypervirulent *Klebsiella pneumoniae*, Singapore*

Name	Sequence
K2_wcaJ Up F	TATGACATGATTACGAATTCAGCTCTGGCTGGTCCACTTA
K2_wcaJ Up R	AGTTTTTCTCACATTTAAGCTGCGAACG
K2_wcaJ Down F	AAATGTGAGAAAACTCTTAGTGTTGCCATGA
K2_wcaJ Down R	CTTGATGCCTGCAGACGCGAGAATGGAATTGTTC
K2_wcaJ Check F	GGTTGAAAACGGAGACGGTA
K2_wcaJ Check R	CGTTGTTGCGAGTCATTCAG
K5_wcaJ Up F	TATGACATGATTACGAATTCTATCTGGAAGACTGGCACGA
K5_wcaJ Up_R	CGCGGAATGACATGCATAACCTCAAATCAATC
K5_wcaJ Down_F	TGCATGTCATTCCGCGTTGTTCAATTTCT
K5_wcaJ Down_R	CTTGATGCCTGCAGAGCTCTGGCTGGTCCACTTA
K5_wcaJ Check_F	TTTTAGTTTTGTAACCTATGGCAGTT
K5_wcaJ Check_R	CCGATCTGTTGCTTGGACAT

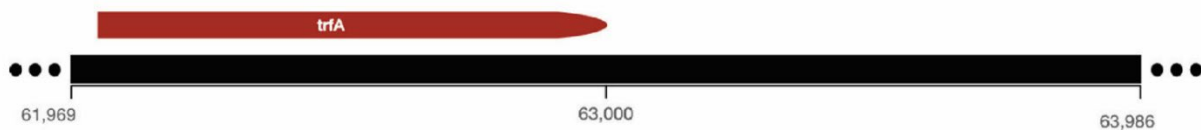
*F, forward; R, reverse.



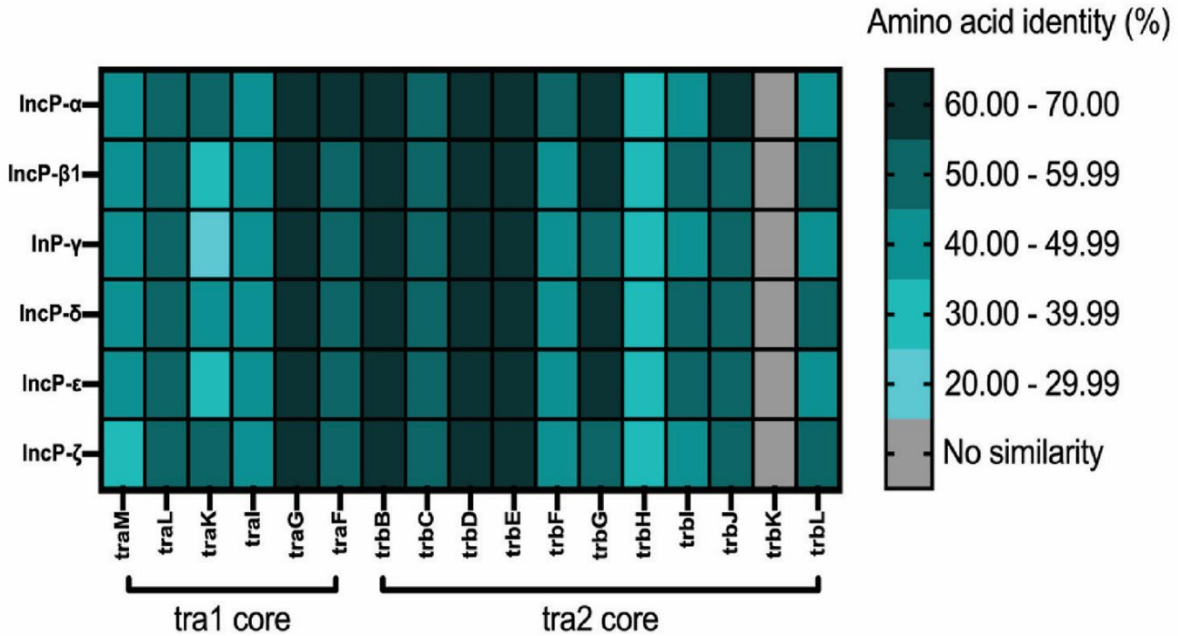
Appendix 2 Figure 1. Distribution of *blaKPC* and *blaNDM* plasmids in the Carbapenemase-Producing *Enterobacteriales* in Singapore collection, 2010–2015. A) Percentage of isolates belonging to *blaKPC* dominant cluster or *blaNDM* dominant cluster in each year. B) Distribution of *blaKPC* dominant cluster (pKPC2), *blaKPC* nondominant cluster (other non-pKPC2 *blaKPC* plasmids), *blaNDM* dominant cluster (pNDM1), and *blaNDM* nondominant cluster (other non-pNDM1 *blaNDM* plasmids) in numerous ST sequence types of *Klebsiella pneumoniae* strains (I–IV), *Escherichia coli* (V–VIII), and *Enterobacter cloacae* (IX–XII). Each slice in pie chart indicates 1 unique ST. Undefined STs indicate strains that could not be assigned to an ST. ST, sequence type.



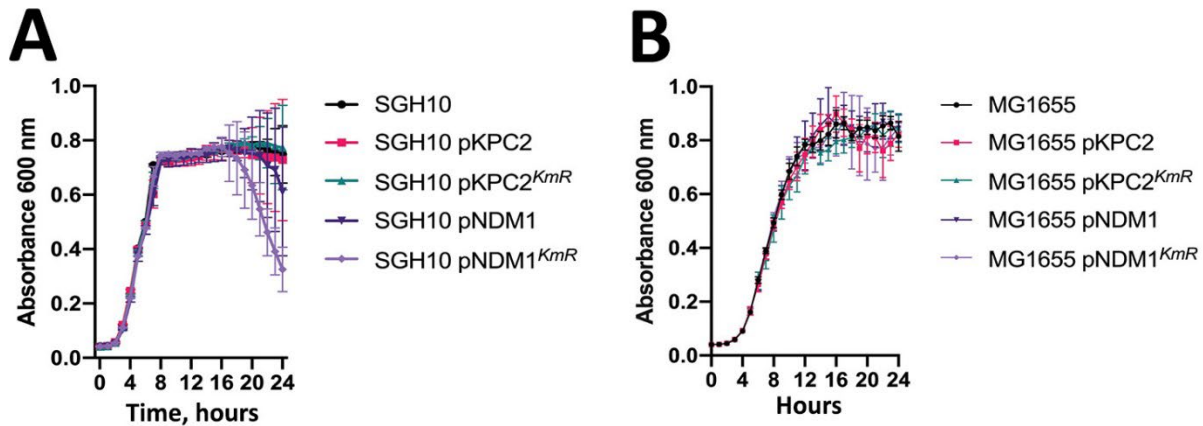
Appendix 2 Figure 2. Downstream *trfA* gene sequence detected in carbapenemase-encoding plasmids in clinical *Enterobacteriales* isolates and hypervirulent *Klebsiella pneumoniae*, Singapore. The *trfA* gene was detected in pKPC2 containing 9 17-bp repeats (blue highlighting) with similarity to the 5 17-bp repeats in the pRK2 oriV sequence. The 17-bp repeats of $T/CGACAT^A/T^G/AAGGTACG^C/T$ were detected downstream of *trfA* gene, which resembled the pRK2 oriV repeats of $TGACA^C/A^T/C^GAGGGGC^A/G^G/C$. Image was generated by using SnapGene (<https://www.snapgene.com>).



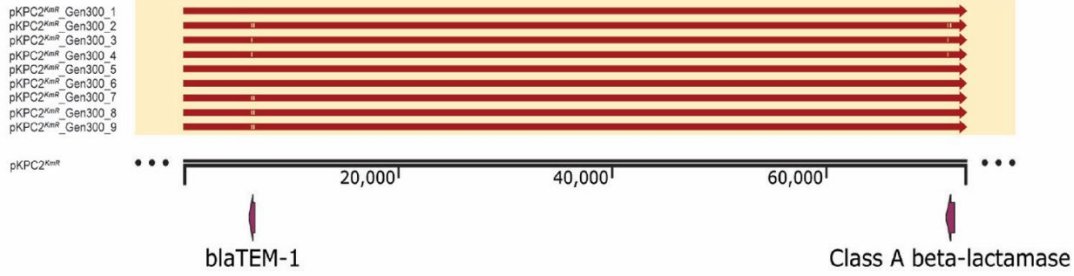
Appendix 2 Figure 3. Replicative pKPC2 fragment detected in carbapenemase-encoding plasmids in clinical *Enterobacteriales* isolates and hypervirulent *Klebsiella pneumoniae*, Singapore. The *trfA* gene and the iteron (a total of 2,018 bp) was cloned by PCR by using forward primer TAAGCAGGATCCGATTACATTGCTGAGAATA TCCAGTATTTAAA TAC; and reverse primer TGCTTAGGATCCAATTTAGAACATTCGAAAAATGATCCAA TTTCGCAT and then inserted into pR6K after *Bam*HI digestion. The fusion plasmid was transformed into *Escherichia coli* Stellar-competent cells. The insertion sequence was verified by Sanger sequencing by using isolated plasmids from successfully transformed cells.



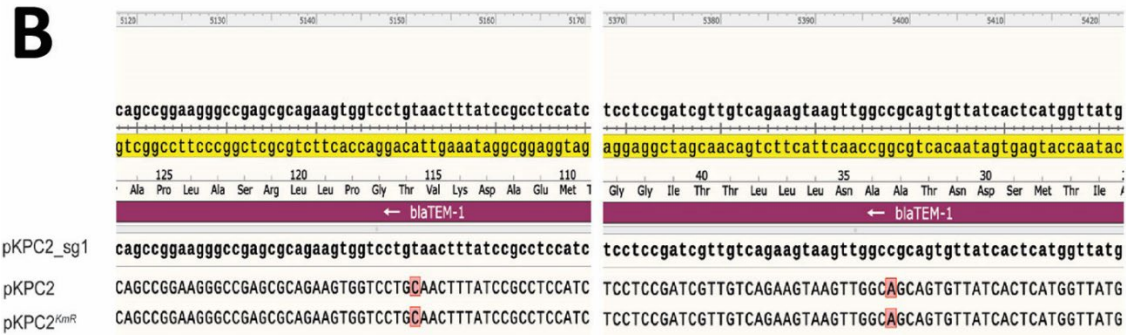
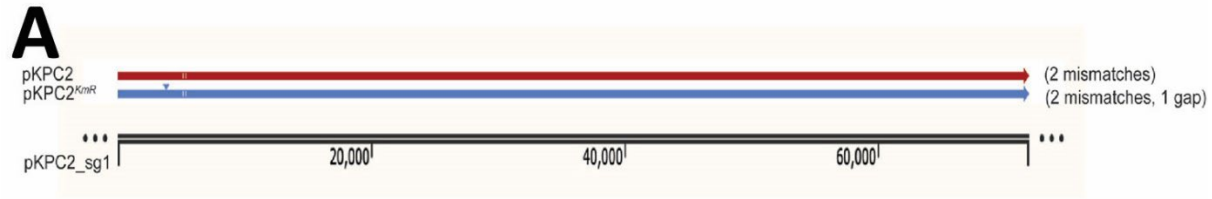
Appendix 2 Figure 4. Heatmap comparing the conjugative genes of pKPC2 to the distinct conjugative genes from IncP in carbapenemase-encoding plasmids from clinical *Enterobacteriales* isolates and hypervirulent *Klebsiella pneumoniae*, Singapore. The protein sequence of the pKPC2 conjugative genes was compared with the IncP plasmids' conjugative genes (*tra1* and *tra2* cores) by using BlastP (<https://blast.ncbi.nlm.nih.gov>). The heatmap shows amino acid percent identity from each comparison.



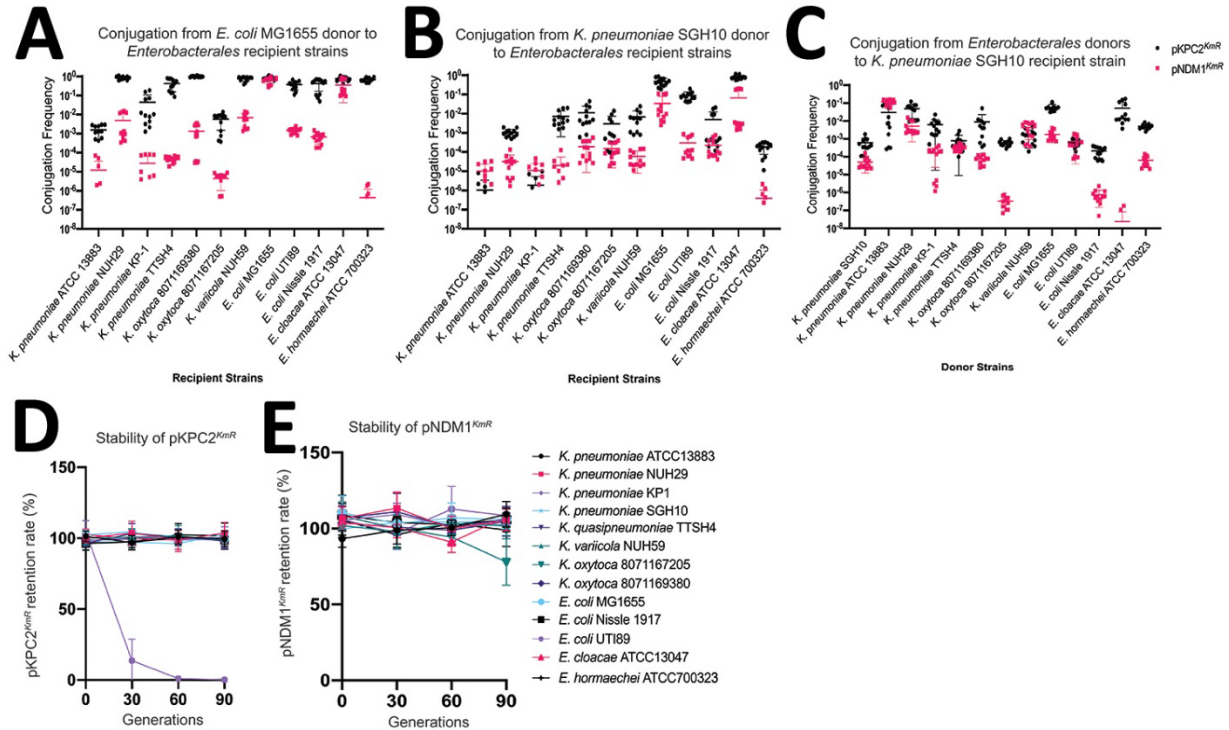
Appendix 2 Figure 5. Growth curve of carbapenemase-encoding plasmids in clinical *Enterobacteriales* isolates and hypervirulent *Klebsiella pneumoniae*, Singapore. A) Representative growth curve of *K. pneumoniae* SGH10. B) Representative growth curve of *E. coli* MG1655. SGH10 and MG1655 were grown with or without plasmids (pKPC2, pKPC2^{KmR}, pNDM1, pNDM1^{KmR}) in M9 media supplemented with 0.4% glucose and 0.4% casamino acids for 24 hours at 37°C. Symbols indicate mean; error bars denote standard deviation.

A**B**

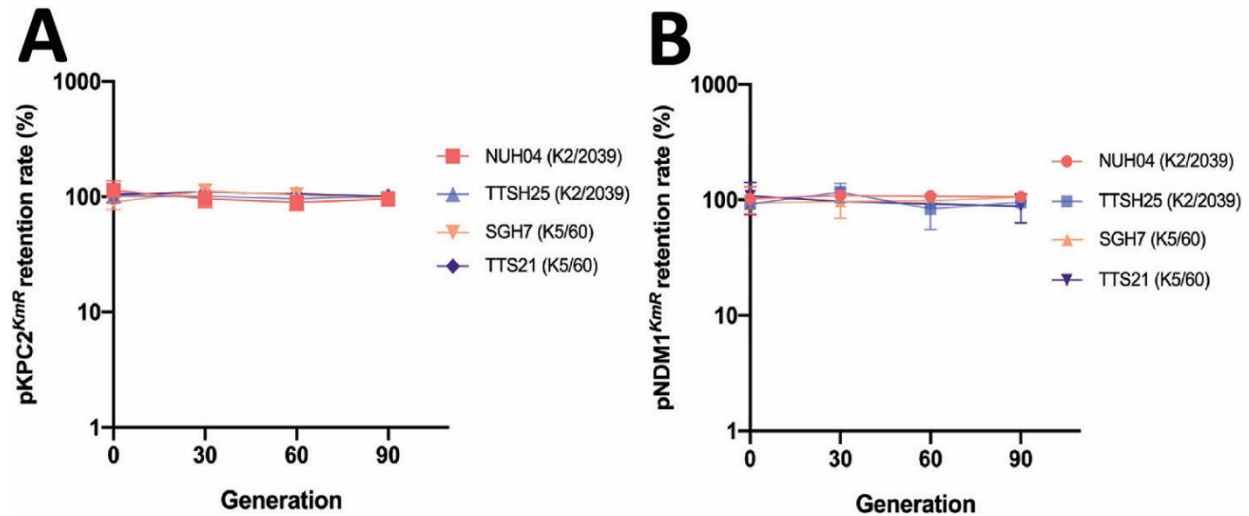
Appendix 2 Figure 6. Sequence comparison between carbapenemase-encoding plasmids in clinical *Enterobacteriales* isolates and hypervirulent *Klebsiella pneumoniae*, Singapore. Multiple pKPC2^{KmR} were isolated from *K. pneumoniae* SGH10 grown over 300 generations (pKPC2^{KmR}_Gen300) and compared with the original pKPC2^{KmR}. A) Sequence alignments of pKPC2^{KmR} and pKPC2^{KmR}_Gen300. White gaps on the red bars indicate single nucleotide mismatch. B) Identified nucleotide mismatches over multiple comparisons. Red highlights indicate positions of the nucleotide mismatch identified in pKPC2^{KmR}_Gen300.



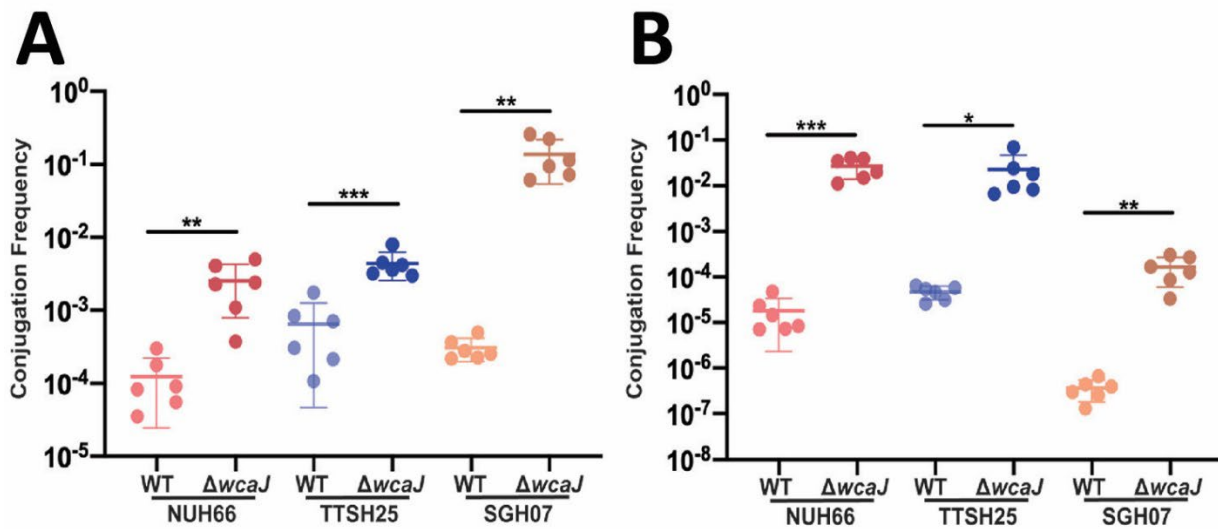
Appendix 2 Figure 7. Sequence comparison between pKPC2, pKPC2^{KmR}, and pKPC2_sg1 (GenBank accession no. MN542377) detected in carbapenemase-encoding plasmids in clinical *Enterobacteriales* isolates and hypervirulent *Klebsiella pneumoniae*, Singapore. A) Comparison between the pKPC2 and pKPC2^{KmR} plasmids from this study with the pKPC2_sg1 plasmid from clinical isolate ENT494. Plasmid alignment showed 2 mismatches (white lines on the red and blue bars) on bla_{TEM-1} gene of pKPC2 and pKPC2^{KmR} compared with pKPC2_sg1. One gap (indicated by the blue arrowhead) was identified on pKPC2^{KmR} corresponding to the kanamycin gene insertion. B) Nucleotide sequence of the 3 plasmids showing the position of the mismatches (T>C at position 5151 and C>A at position 5398 of the pKPC2_sg1 sequence). Both mismatches were on bla_{TEM-1} gene.



Appendix 2 Figure 8. Conjugation frequency and stability of pKPC2^{KmR} and pNDM1^{KmR} among various clinical *Enterobacteriales* isolates and hypervirulent *Klebsiella pneumoniae*, Singapore. A–C) Conjugation frequency of pKPC2^{KmR} and pNDM1^{KmR} from *E. coli* MG1655 donor strain (A) and from *K. pneumoniae* SGH10 donor strain (B) to a panel of *Enterobacteriales* recipient strains; and C) from the panel of *Enterobacteriales* donor strains to *K. pneumoniae* SGH10 recipient strain. Each symbol represents 1 experimental replicate with a total of 12 replicates. Data points that are not seen on the graphs indicate no detectable transconjugant. D,E) Stability of pKPC2^{KmR} (D) and pNDM1^{KmR} (E) in various *Enterobacteriales* strains grown in lysogeny broth up till generation 90. Symbols indicate mean; error bars indicate SD from 3 independent experiments.



Appendix 2 Figure 10. Plasmid stability in low conjugating hypervirulent *Klebsiella pneumoniae* strains in a study of carbapenemase-encoding plasmids in clinical *Enterobacteriales* isolates and hypervirulent *Klebsiella pneumoniae*, Singapore. A,B) Stability of pKPC2^{KmR} (A) or pNDM1^{KmR} (B) in low conjugating hypervirulent *K. pneumoniae* A-KLASS isolates via continuous culture in lysogeny broth for 90 generations. Error bars indicate mean \pm SD from 3 independent experiments.



Appendix 2 Figure 11. Conjugation frequency of carbapenemase-encoding plasmids in clinical *Enterobacteriales* isolates and hypervirulent *Klebsiella pneumoniae*, Singapore. A) Conjugation of pKPC2^{KmR}, pKPC2^{KmR}, and pNDM1^{KmR} to capsule null mutant of low conjugating hypervirulent *K. pneumoniae* strains. B) Conjugation of pNDM1^{KmR} from *Escherichia coli* MG1655 to NUH66, TTSH25, or SGH07 wildtype strains and capsule null mutant ($\Delta wcaJ$). Error bars indicate mean \pm SD from 3 independent experiments. * $p < 0.05$; ** $p < 0.01$; *** $p < 0.001$.